ESTUDIO DE GRIETAS TRANSVERSALES Y DE DELAMINACIÓN EN LAMINADOS SIMÉTRICOS [0/90] DE MATERIAL COMPUESTO USANDO LA FORMULACIÓN DE INTERFASE ELÁSTICA LINEAL-FRÁGIL

STUDY OF TRANSVERSAL AND DELAMINATION CRACKS IN [0/90] SYMMETRIC LAMINATES BY MEANS OF THE LINEAR ELASTIC BRITTLE INTERFACE FORMULATION

L. Távara, V. Mantič, A. Blázquez, E. Graciani, F. París

Grupo de Elasticidad y Resistencia de Materiales,
Escuela Técnica Superior de Ingenieros, Universidad de Sevilla,
Camino de los Descubrimientos s/n, 41092 Sevilla, España.
E-mail: ltavara@esi.us.es, mantic@esi.us.es, abg@esi.us.es, graciani@esi.us.es, paris@esi.us.es

RESUMEN

En el presente trabajo se estudia el inicio y crecimiento de grietas transversales y de delaminación en laminados simétricos [0/90], bajo cargas de tracción en la dirección de las fibras en las láminas externas. El problema se resuelve con un código basado en el Método de los Elementos de Contorno (MEC) y usando una nueva formulación de interfase elástica lineal-frágil (IELF). Esta formulación incluye una ley de comportamiento elástica lineal-frágil en la interfase que permite el uso de un criterio de fallo en modo mixto. La formulación IELF ha demostrado que puede ser usada para estudiar y caracterizar el comportamiento de las diferentes grietas de interfase que aparecen en este problema. El sistema de materiales usado en este problema es un laminado de fibra de carbono con matriz epoxi (AS4/8552 Hexcel) $[0_3/90_3]_S$. Los resultados numéricos muestran que la formulación IELF implementada en el código MEC es una herramienta útil y eficiente para describir el comportamiento de las grietas transversales y de delaminación en laminados simétricos [0/90].

ABSTRACT

This paper studies transversal and delamination crack onset and growth in [0/90] symmetric laminates under traction loads in the fibre direction of the external laminas. The problem is solved by means of a Boundary Element Method (BEM) code and using a new Linear Elastic Brittle Interface (LEBI) formulation. This formulation includes a linear elastic-brittle constitutive law in the interface that allows the use of a mixed mode failure criterion. The LEBI formulation has proved to be capable to study and characterize the behaviour of the different interface cracks involved in this problem. The material system used is carbon fibre reinforced polymer laminate with epoxy matrix (AS4/8552 Hexcel) $[0_3/90_3]_S$. Numerical results show that the LEBI formulation implemented in a BEM code is a useful and efficient tool able to describe the transversal and delamination cracks behaviour in [0/90] symmetric laminates.

PALABRAS CLAVE: Composites, Delamination, Mixed mode fracture, Interface crack

1. INTRODUCTION

Composites are experiencing a massive use in primary structures of commercial aeroplanes. The associated current demand for diminishing weight requires a better knowledge of mechanisms of failure. An essential step is to generate physically based failure or damage criteria. All this leads to the necessity of revisiting classical problems of composite laminates such as the mechanism of damage in $[0/90]_S$ laminates [1].

In the present work the linear elastic-brittle interface (LEBI) model developed in Távara *et al.* [2, 3] has been enhanced, resulting in a linear elastic-brittle constitutive law that takes into account the variation of the fracture toughness with the fracture mode mixity. The constitutive law considers the possibility of linear elastic frictionless contact between fibre and matrix once a portion of the interface is broken. The LEBI model has been implemented in a 2D collocational BEM code.

The present paper is a step forward towards the characterization of the mechanisms of failure of a $[0/90]_S$ laminate. Its aim is to characterize the behaviour of the two types of crack involved in the problem (transverse and delamination) by means of the LEBI formulation, trying to connect predictions with the observed damage of specimens, as shown in [4].

2. DESCRIPTION OF THE PROBLEM

The problem analyzed is shown in Fig. 1. It represents a $[0/90]_S$ laminate under tensile loading in the direction of the 0° fibres, that was solved previously by means of the BEM and using the Virtual Crack Closure Technique (VCCT) to calculate the Energy Release Rate (ERR) by Blázquez *et. al.* [5, 6] and by París *et. al.* [1].

The first damage in this laminate is expected to be the nucleation and growth of cracks in the 90° ply transverse to the load. When one of these cracks approaches the inter-

face with the 0° ply, it is accepted that it stops. New transverse cracks appear in the 90° ply with increasing load until the crack density reaches a critical value. Transverse matrix cracking in 90° ply leads to a load redistribution in the adjacent 0° plies and induces local stress concentrations at the neighborhood of the crack tips that, when the tips are near to the interface, can involve significant interlaminar delamination [1, 7].

For the case analyzed in this work, the material systems is a carbon–epoxy (AS4/8552 Hexcel) laminate $[0_3/90_3]_S$, direction 1 being considered the fibre direction: E_{11} = 45.6 GPa, $E_{22} = E_{33}$ = 16.2 GPa, $\nu_{12} = \nu_{13}$ = 0.278, ν_{23} = 0.4, $G_{12} = G_{13}$ = 5.83 GPa, G_{23} = 5.786 GPa. The half-thickness of the set of 90° ply, t, and the thickness of each of the set of 0° plies is 0.55 mm. The average separation between transverse cracks is taken to be $2L$ = 4 mm.

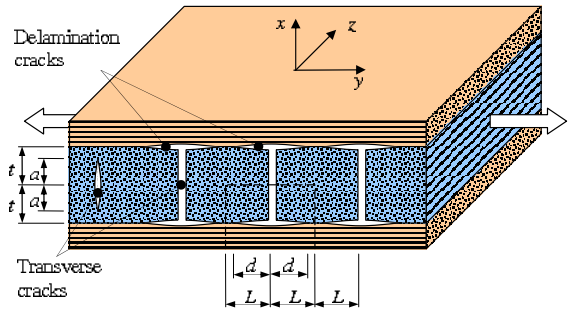

Figure 1: Transverse and delamination cracks in $[0/90]_S$ laminate, taken from [1].

3. MODEL OF THE PROBLEM

The previously described problem that will be studied, has some usually accepted damage patterns [1], see Fig. 2. One having only a transverse crack Fig. 2(a) and (b), the second having a transverse crack that has reached the interface with the 0° lamina and has deflected, starting a symmetric delamination Fig. 2(c). The third damage pattern shown Fig. 2(d) indicates that delamination will start to appear before the transverse crack reaches the interface. This scheme represented in Fig. 2(d) is known in Fracture Mechanics as the Cook-Gordon mechanism [8].

As mentioned before, the LEBI model is used to study the present problem. The cases shown in Fig. 2 exhibit symmetry (with respect to the horizontal middle plane in the figure), this fact allows us to study the delamination crack growth either using the configuration shown in Fig. 3(a) or Fig. 3(b). Nevertheless, if we want to study the onset and growth of the transversal crack (modeled using the LEBI model), it is necessary the use of the configuration presented in Fig. 3(a) because of the use of interface elements that, in the present implementation, needs the presence of both solids adjacent to the interface.

In the BEM model used to simulate the geometry shown in Fig. 3(a) the uniform boundary element mesh has 3860

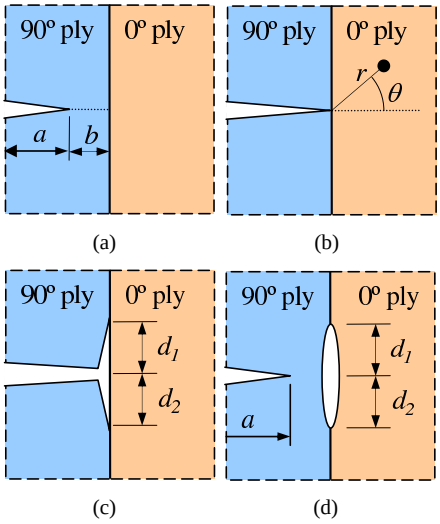

Figure 2: Damage configurations considered with a transverse crack: (a) not reaching the interface, (b) terminated at the interface, (c) deflected at the interface, and (d) approaching a damaged interface (mechanism of Cook-Gordon). Slightly modified version of a picture from [1].

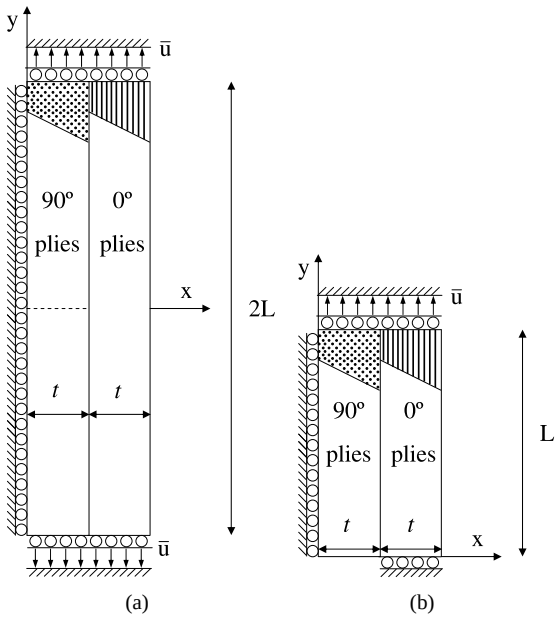

Figure 3: Geometry and boundary conditions for the delamination problem in [0/90] symmetric laminates.

linear elements, while in the other case (Fig. 3(b)) the mesh is formed by 2040 linear elements. In both cases the constant element size is 5μm.

4. NUMERICAL RESULTS FOR TRANSVERSE AND DELAMINATION CRACKS

4.1. Transverse cracks

As mentioned before, to study the onset and growth of the transverse crack, the geometry shown in Fig. 3(a) is used.

The LEBI elements have been included at the interface between the 0° ply and 90° ply, and also in the assumed crack path of the transverse crack that could appear in the 90° ply (shown in Fig. 3(a) with a dashed line).

The properties of the interfaces at the two positions (transversal or delamination) were considered to be different, see Table 1.

Table 1: Considered combinations of the interface properties in the delamination problem of [0/90] symmetric laminates.

Position	G_{Ic}(Jm^{-2})	$\bar{\sigma}_c$(MPa)	k_n (MPa/μm)
transversal	75	61	24.807
delamination	75	90	54

Notice that the fracture toughness in mode I, G_{Ic}, is considered to be the same in both positions, but the critical stress, $\bar{\sigma}_c$, varies leading to different values of k_n. Finally, the ratio $k_n/k_t = 3$ is considered.

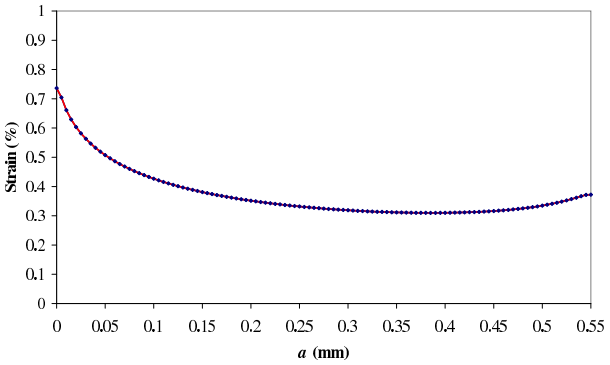

Figure 4: Applied strain versus the length of the transverse crack a.

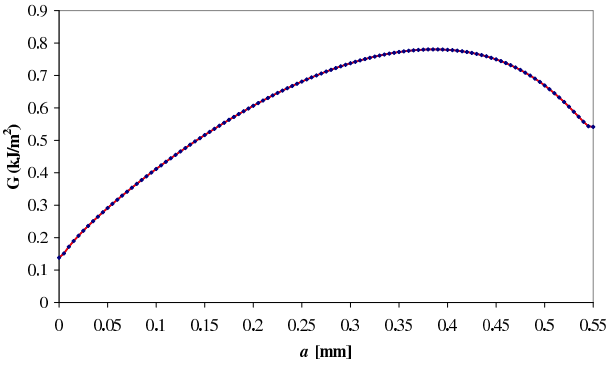

Figure 5: Predictions of the ERR (G), for a fixed applied strain of 1 %, versus the length of the transverse crack a.

In Fig. 4 the actual applied average (longitudinal) strain, $\varepsilon = \bar{u}/L$, versus the length of the transverse crack a is plotted. It can be seen that once a critical strain is applied the crack grows in an unstable manner (less applied strain is needed) until it reaches the interface between the 0° ply and 90° ply.

Although it is not shown in the above mentioned figure the fracture energy G_c was always equal to $G_{Ic} = 75\text{Jm}^{-2}$, due to the mode I behavior of the transversal crack and according to Table 1.

Fig. 5 represents the distribution of the values of the ERR at the crack tip of the growing transverse crack versus the length a, for a fixed applied strain of 1 %.

4.2. Delamination cracks

In the following, the onset and growth of the delamination crack is studied. In particular the effects of the variation of the geometry to be used and the consideration or not of an elastic contact algorithm are elucidated in the following section.

4.2.1. Different geometries

To study the onset and growth of the delamination crack, the geometries shown in Fig. 3(a) and (b) are used. The properties correspond to the ones shown in Table 1. The contact algorithm is also activated.

In Fig. 6, a comparison of the actual applied strain versus the length of the delamination crack d is plotted, for the two geometries shown in Fig. 3. In fact, the value of d represents, half of the total length of the delamination crack. For the geometry shown in Fig. 3(b) is $d = d_1$, while for Fig. 3(a) d is defined as $d = (d_1 + d_2)/2$. The reason for this definition is that d_1 is not necessarily equal to d_2, as sometimes in modeling a crack growth it is possible to obtain non-symmetric solutions of originally symmetric problems. The growth of the delamination crack is an example of this behavior. Fig. 7 represents a comparison of the variations of the fracture energy necessary to cause the crack growth versus the length d; while Fig. 8 shows a comparison of the variations of the values of the ERR of the transverse crack versus the length a, for a fixed applied strain of 1 %, for the two geometries shown in Fig. 3. In Figs. 6-8 comparisons of the results

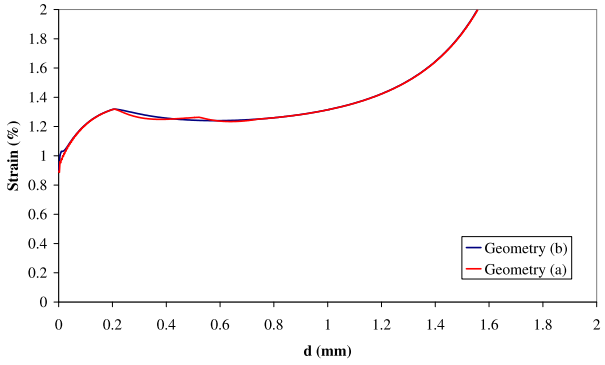

Figure 6: Comparison of the applied strain versus the length of the delamination crack d, for the geometries shown in Fig. 3.

for the onset and growth of the delamination crack obtained by using the two geometries shown in Fig. 3 are

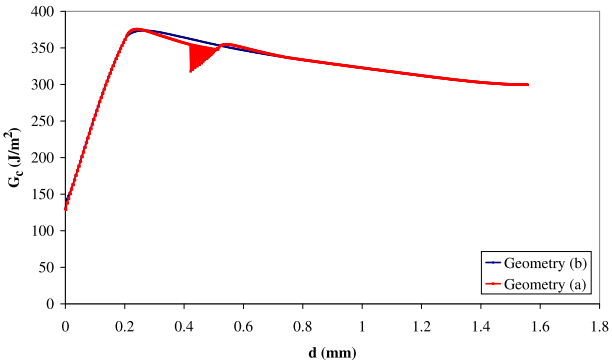

Figure 7: Comparison of the distribution of the fracture toughness, energy necessary to cause the crack growth, versus the length d, for the geometries shown in Fig. 3.

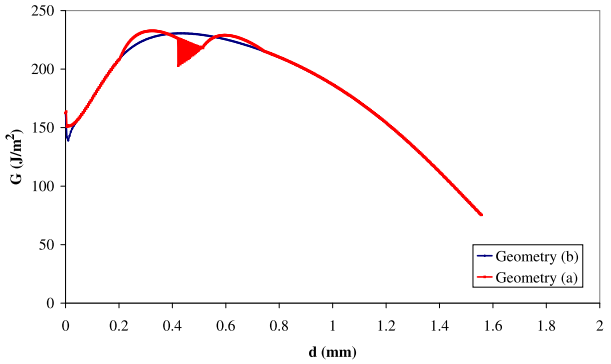

Figure 8: Comparison of the predictions of the ERR (G), for a fixed applied strain of 1 %, versus the length of the delamination crack d, for the geometries shown in Fig. 3.

presented. As can be seen from these figures, the results for geometry shown Fig. 3(a) presents some spurious oscillations. This fact is caused because although the problem is symmetric, the geometry shown in Fig. 3(a) and the sequentially linear analysis used [2], allow for a non-symmetric crack growth, while in the geometry shown in Fig. 3(b) a symmetric crack growth is assumed. In this manner, once one crack branch (top or bottom) initiates an unstable growth (less applied strain is necessary for crack growing) the crack grows only trough this branch, leading to $d_1 \neq d_2$. Before a continuos unstable growth initiates in the second branch, some spurious behavior is obtained caused because the crack grows in both branches alternating small advances in both crack branches, see Figs. 7-8. In particular, picks and valleys obtained in Fig. 6 for the geometry shown in Fig. 3(a) are related to the unstable growth of one branch followed by the unstable growth of the other branch. Nevertheless, this behavior is observed along the unstable growth zone only, and once the crack growth becomes stable the symmetry of the problem is recovered. Thus, in the following to avoid this spurious behavior (with no clear physically meaning), with the aim to reduce computing time and because the obtained results are very similar, only the geometry shown in Fig. 3(b) will be used in the following. In any case the observed alternating crack growth will require a further and more extensive study in the future.

4.2.2. Contact influence

The delamination crack starts being an open crack and, after a certain crack length size is reached, it starts to be partially in contact. Thus, the influence of contact in this specific problem is studied. In one case, once the LEBI element is broken it may enter in frictionless contact [9]. In the other case interpenetration is allowed without causing any contact stresses. Again the properties taken where the ones defined in Table 1 and the geometry used is the one shown in Fig. 3(b).

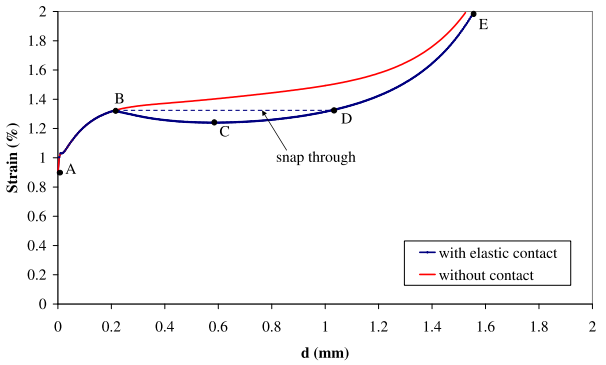

Figure 9: Comparison of the applied strain versus the length of the delamination crack d, considering contact or not.

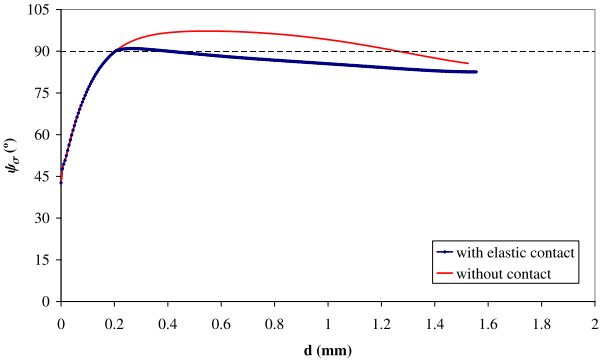

Figure 10: Mixity angle ψ_σ obtained at the crack tip versus the length of the delamination crack d, considering contact or not.

In Fig. 9 a comparison of the actual applied strain versus the length of the delamination crack d is plotted, considering contact or not. Notice that when contact is considered the delamination crack initially behaves in a stable manner, then a relatively large unstable growth appears where an instability phenomenon called snap-through takes place, and finally a stable growth is reached again. If contact is not considered, allowing overlapping of delamination crack faces, the crack growth is always stable.

Fig. 10 represents a comparison of the mixity angle ψ_σ, ($\psi_\sigma = \tau/\sigma$) [9], obtained at the crack tip versus the length of the delamination crack d. In a first stage a stable crack

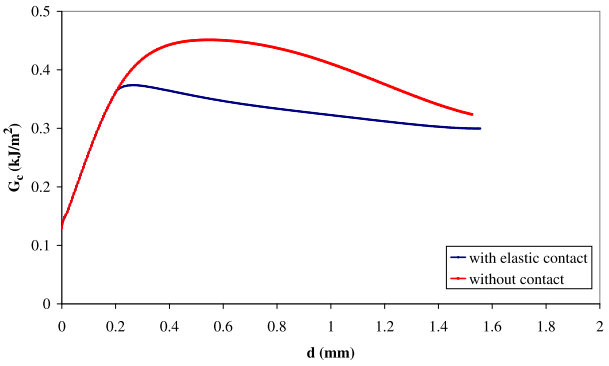

Figure 11: Comparison of the distribution of the fracture toughness, energy required to cause the delamination crack growth, versus the length d, considering contact or not.

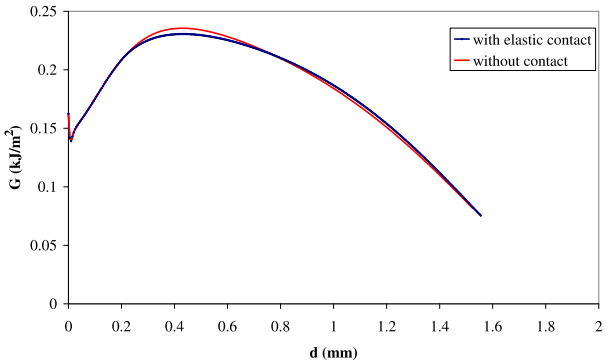

Figure 12: Comparison of the predictions of the ERR (G), for a fixed applied strain of 1 %, versus the length of the delamination crack d, considering contact or not.

growth in mixed mode ($\psi_\sigma \leq 90°$) is observed for two cases. After this stage a great difference of ψ_σ values is obtained. When contact is considered, a small stage of crack growth with the crack tip closed appears, and after this small stage the crack grows in mixed mode again, with the crack tip opened forming a "bubble" near the crack tip. On the other hand, when contact is not considered, the stage of crack growth with the crack tip closed is very large.

Fig. 11 represents a comparison of the distribution of the fracture energy necessary to cause the crack growth versus the length *d*. In this case it is noteworthy that when contact is considered the fracture energy necessary to growth is less than when contact is not considered. Thus, contact makes easier crack propagation. This fact could be explained because of the failure criteria used. As detailed in [9], when the crack tip is in compression it needs more energy (greater tangential stresses which control the failure in this problem) to growth.

Fig. 12 shows a comparison of the distribution of the values of the ERR of the delamination crack versus the length *d*, for a fixed applied strain of 1 %. It can be seen that, the differences of the values of the ERR of the delamination crack are almost negligible if contact is considered or not.

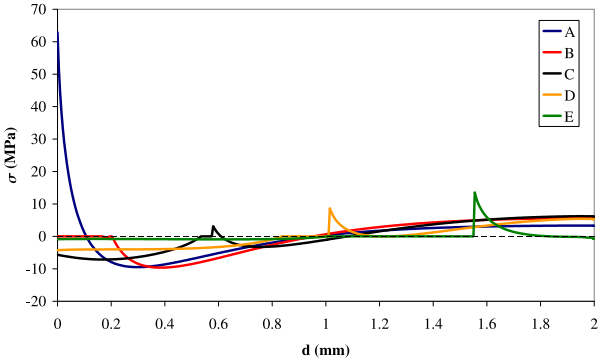

Figure 13: Normal stresses obtained at the interface between 0° and 90° plies for the different load steps shown in Fig. 9.

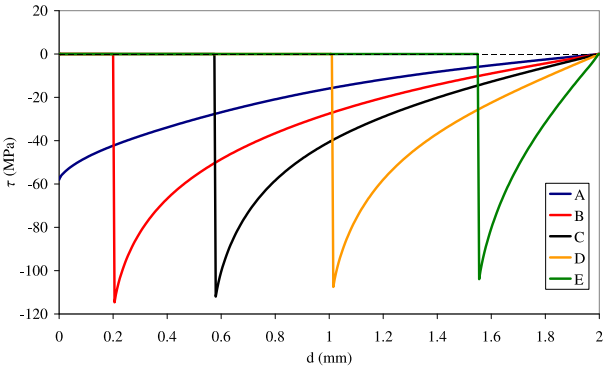

Figure 14: Tangential stresses obtained at the interface between 0° and 90° plies for the different load steps shown in Fig. 9.

In Fig. 13 and Fig. 14 the normal and tangential stresses at the interface between 0° and 90° plies are plotted for different load steps shown in Fig. 9 when elastic contact is considered. As can be seen from these figures the tangential stresses are much larger than the normal stresses during the delamination crack growth. In particular in Fig. 13, the "bubble" formed near the crack tip can be observed ($\sigma = 0$). In Fig. 15 the deformed shapes for the same load steps considered in Fig. 13 and Fig. 14 are shown. These deformed shapes are multiplied by 20 only in the *x*-direction.

5. CONCLUSIONS

As shown by the numerical results presented in this work, the LEBI formulation seems to be a promising tool to describe the behavior of the transversal and delamination cracks in [0/90] symmetric laminates. As shown by the realistic results presented, the BEM tool developed can be considered a useful tool, due to the fact that the crack propagation can be modeled by using the same uniform mesh. While for the VCCT [1, 10] a refined mesh is necessary near the crack tip, thus for different load steps,

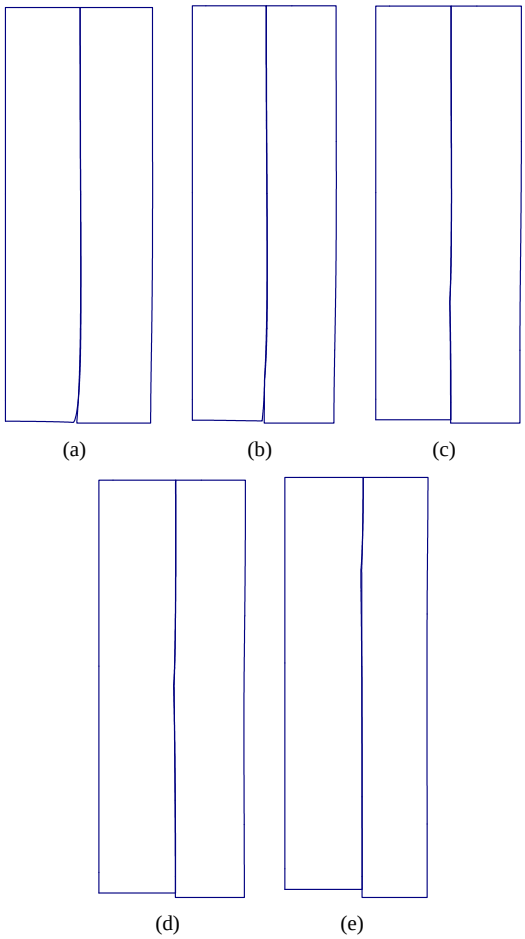

Figure 15: Deformed shapes obtained for the different load steps shown in Fig. 9, multiplied by 20 in the x-direction only.

different meshes are needed. It is remarkable that the onset and unstable growth of the transversal crack requires a significatively lower load (applied strain) than the one needed to the onset of the delamination crack. In all the analyzed cases, the transversal crack reached the interface between 0° and 90° plies before the delamination crack onset. Once the delamination crack starts to growth three stages can be clearly identified: (i) initial stage - initially a relatively short stable growth of the delamination crack takes place with open traction-free crack faces; (ii) intermediate stage - the delamination crack growth becomes unstable and there is contact between the crack faces, except for the zone close to the crack tip where a kind of bubble appears; (iii) final stage - the delamination crack growth becomes stable again. It is interesting to notice that although the problem configuration (geometry, material and boundary conditions) is symmetric its solution including a transversal and delamination crack may be non-symmetric. This fact was observed in the second stage of the delamination crack growth (unstable), where an non-symmetric growth can be observed in the two branches of the delamination crack.

ACKNOWLEDGEMENTS

The work was supported by the Junta de Andalucía (Projects of Excellence TEP-1207, TEP 02045 and P08-TEP 04051), the Spanish Ministry of Education and Science through Project TRA2006-08077 and MAT2009 - 140022.

REFERENCES

[1] F. París, A. Blázquez, L. N. McCartney, and V. Mantič. Characterization and evolution of matrix and interface related damage in $[0/90]_S$ laminates under tension. Part I: Numerical predictions. *Composites Science and Technology*, 70:1168–1175, 2010.

[2] L. Távara, V. Mantič, E. Graciani, J. Cañas, and F. París. Analysis of a crack in a thin adhesive layer between orthotropic materials. An application to composite interlaminar fracture toughness test. *Computer Modeling in Engineering and Sciences*, 58(3):247–270, 2010.

[3] L. Távara, V. Mantič, E. Graciani, and F. París. BEM analysis of crack onset and propagation along fiber-matrix interface under transverse tension using a linear elastic-brittle interface model. *Engineering Analysis with Boundary Elements*, 35:207–222, 2011.

[4] F. París, A. Blázquez, L. N. McCartney, and A. Barroso. Characterization and evolution of matrix and interface related damage in $[0/90]_S$ laminates under tension. Part II: Experimental evidence. *Composites Science and Technology*, 70:1176–1183, 2010.

[5] A. Blázquez, V. Mantič, F. París, and L. N. McCartney. Stress state characterization of delamination cracks in [0/90] symmetric laminates by BEM. *International Journal of Solids and Structures*, 45:1632–1662, 2008.

[6] A. Blázquez, V. Mantič, F. París, and L. N. McCartney. BEM analysis of damage progress in 0/90 laminates. *Engineering Analysis with Boundary Elements*, 33:762–769, 2009.

[7] JM. Berthelot. Transverse cracking and delamination in cross-ply glass-fiber and carbon-fiber reinforced plastic laminates: static and fatigue loading. *Applied Mechanics Reviews*, 56:111–147, 2003.

[8] J. Cook, J. E. Gordon, C.C. Evans, and D.M. Marsh. A Mechanism for the Control of Crack Propagation in All-Brittle Systems. *Proceedings of the Royal Society of London. Series A, Mathematical and Physical Sciences*, 282:508–520, 1964.

[9] L. Távara. *Damage initiation and propagation in composite materials. Boundary element analysis using weak interface and cohesive zone models*. PhD Thesis. Universidad de Sevilla: Sevilla, 2010.

[10] A. Blázquez. Transversal and delamination crack onset and growth in $[0/90]_S$ laminates. *GERM Private Comunication*, 2010.